Hindawi
Geofluids
Volume 2022, Article ID 3078233, 10 pages
https://doi.org/10.1155/2022/3078233

Research Article

Extension Limit of a Straight-Swirling Mixed Jet Bit and Its Influential Factors in Radial Jet Drilling

Peng Du, Weikang Xia, and Chaoxiong Yu

School of Mechanical Engineering, Anhui University of Science and Technology, Huainan 232001, China

Correspondence should be addressed to Peng Du; dpeng@aust.edu.cn

Received 3 April 2022; Revised 9 May 2022; Accepted 11 May 2022; Published 23 May 2022

Academic Editor: Yong Li

Radial jet drilling (RJD) is applied to low-permeability and unconventional natural gas. A self-propelled bit chiefly affects the borehole length and drilling efficiency. Herein, for a straight-swirling mixed jet (SSMJ) bit, a prediction model of the drilling extension limit L_{EL} was established by analysing the forces and pressure loss of RJD system. L_{EL} of a specific project was calculated and the pressure loss and forces distribution were obtained. Additionally, the influence laws of the main factors on L_{EL} were studied using the established model. The results indicated that the high-pressure hose contributes the main system pressure loss, and the recoil force of backward nozzles is the sole driving force of RJD. The recoil force of forward nozzle and friction between the hose and borehole constitute the main resistances. Increasing the pump pressure p_b, backward nozzle diameter d_b, and jet diffusion angle θ_x and reducing forward nozzle diameter d_f, impeller central hole diameter d_m, and backward nozzle inclination angle θ_b are conducive to improving L_{EL}. However, larger p_b and d_b increase the hydraulic consumption, besides larger θ_x or smaller d_f, and d_m will reduce the rock-breaking capability. From a sensitivity analysis, p_b and d_m have the maximum and minimum influence on L_{EL}, respectively. Finally, prediction value L_{EL} of an oil well in Eastern Sichuan can be up to 63.7 m. The results provide a guidance for the hydraulic parameters and key component selection, additionally bit structure optimization of RJD.

1. Introduction

China is rich in unconventional natural gas resources of coalbed methane (CBM) and shale gas, etc. [1]. Of these, the total CBM resources in China that are within 2000 m from the ground are estimated to be 36.81 trillion cubic meters [2, 3]. Most of the production wells are located in the southern Qinshui Basin and eastern Ordos Basin [4, 5]. Radial jet drilling (RJD) technology was imposed in the 1980s [6]. The use of RJD to exploit low-permeability oil-gas reservoirs, CBM, and shale gas is a hot topic and an important direction for the development of oil-gas resource drilling [7–10]. A RJD technique utilizes hydraulic energy to create several lateral holes in different directions and levels with several different lengths. These lateral holes are made by milling the casing with a small bit and then extending these holes laterally using high-pressure hydraulic jetting, which can improve the recovery of oil and gas with lower cost [11]. In 2011, Petrobel Company drilled five 50 m radial wells and one 90 m well at two stratums at No.1 well in Belayin Oil Field [12]. The successful application of RJD in the world reflects its promising future.

Predicting the extension limit of the RJD can optimize the layout of boreholes, and it is significant to improve their output. To date, some authors researched the main factors influencing the extension limit, such as the self-propelled force of the bit and system pressure loss. Buset et al. researched the self-propelled force of multiple nozzle jet bits of a RJD system [13]; Ma et al. established a calculation model of pressure loss for RJD system by analysing the pressure loss of a coiled tube and high-pressure hose [14]; Zhang et al. designed a jet radial horizontal drilling simulation experiment system of the casing windowing and evaluated the self-propelled force of a multiorifice nozzle [15].

A self-propelled bit, the "core" of RJD, chiefly affects the borehole length and drilling efficiency. RJD technology changes the direction from a vertical to horizontal direction using a diverter [15]. The turning radius of the interior trail

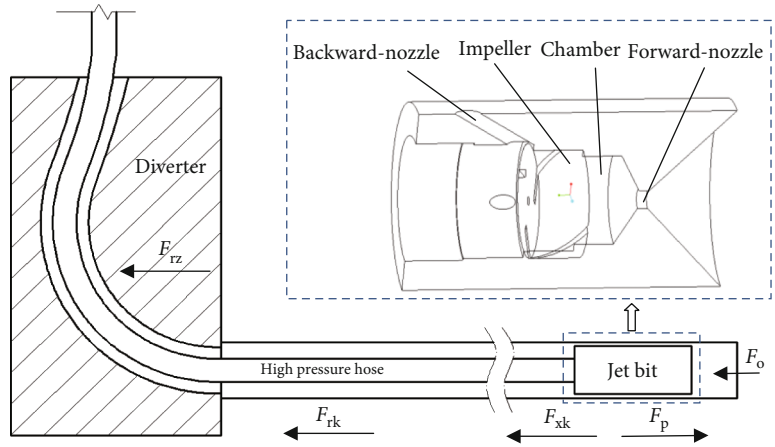

Figure 1: Force model of the RJD system.

within the diverter is small, which limits the dimension of the bit. Therefore, only a simple structure can be selected in the design of bit. Research [16–19] indicated that the jets used for drilling can be divided into three main types: straight, swirling, and a combination thereof. Li et al. researched sandstone-breaking characteristics by experiment and studied the influence of working conditions of lithology, axis length, jet pressure, and standoff distance [20]. Liu et al. adopted the FLUENT combined with RNG turbulence model to analyze the multinozzle jet flow field and study the effects of inclination angle of forward nozzles and standoff distance [21]. Du et al. researched the damage characteristics of straight jet, swirling jet, and SSMJ and then obtained the velocity fields of the three jets by 3DPIV [22]. Overall, a straight jet can drill a deep hole, yet the diameter is smaller because the energy of the jet is more centralized. A swirling jet can be used to drill a larger diameter hole, but it has a boss at the centre owing to the central low-velocity zone of the jet. A combination of a dual-jet nozzle or an SSMJ nozzle can combine the advantages of both a straight jet and swirling jet [23–25]. Few articles have been published on the research on predicting the extension limit of an SSMJ and its influential factors.

With an SSMJ as the research objective, this study established a model to predict the extension limit of a RJD system by analysing the distributions of force and pressure loss. Thereafter, the drilling extension limit of a specific project was calculated and the pressure loss and forces were obtained. Finally, the influence laws of the main parameters (pump pressure, diameter of the forward nozzle and backward nozzles, diffusion angle of the jet, inclination angle of the backward nozzle, etc.) on the extension limit were studied using the established prediction model; additionally, the influence degree of parameters was investigated. We conducted these studies in an attempt to provide a guidance for the construction parameter selection of the RJD.

2. Mathematical Model

During drilling, the horizontal section of the RJD system has a self-propelled force of the bit (F_p), the pressure of an external fluid on the bit (F_o), friction between the diverter and high-pressure hose (F_{rz}), friction between the borehole and high-pressure hose (F_{rk}), and friction between the borehole and bit (F_{xk}), as shown in Figure 1. Owing to the lower flow rate of the system and the use of a pure water jet during operation, the viscosity is low, and the viscous resistance of the fluid in the borehole to the hose is also small, which can be ignored. The resultant force F on the RJD system is expressed as

$$F = F_p - F_o - F_{rz} - F_{rk} - F_{xk}. \quad (1)$$

2.1. Self-Propelled Force of the Bit. An SSMJ bit composes of a body and an impeller with a central hole and several slots (Figure 1). Its basic operating principle is as follows: the fluid flows into the mixing chamber through the central hole and slots of the impeller, generating a low-speed, straight-swirling flow. An SSMJ with a high axial velocity and peripheral rotational intensity is then created successively under the pressurization of the nozzle outlet, and the extended section ensures a specific target distance when breaking rock. In addition, the jets created by the backward nozzles can push the bit and high-pressure hose forward. A straight jet has only a one-dimensional velocity; however, for a swirling jet, the trajectory is approximately a helix, and the velocity of any particle is a space vector, its axial velocity u is parallel to the jet axis, and its radial and tangential velocities v and w are perpendicular to the jet axis [26, 27]. When the system is operating, the forces of the bit include the recoil force of the backward nozzles (F_b) and recoil force of the forward nozzle (F_f). Naturally, the self-propelled force of the bit F_p is F_b minus F_f.

2.1.1. Recoil Force of the Forward Nozzle. The recoil force of the SSMJ forward nozzle was produced from two parts: straight jet and swirling jet. If the forward nozzle and the impeller central hole diameter are d_f and d_m, respectively, the flow area of the swirling jet is the difference between the forward nozzle area and the central hole area, and the equivalent diameter of the swirling jet can be obtained:

$$d_x = \sqrt{d_f^2 - d_m^2}. \quad (2)$$

(a) Recoil Force of the Straight Jet. The equation to calculate the recoil force of the straight jet acting on the bit is [27]

$$F_m = 1.56\mu_f d_m^2 p_i, \quad (3)$$

where p_i is the nozzle inlet pressure (MPa) and μ_f is the flow coefficient of the forward nozzle

(b) Recoil Force of the Swirling Jet. Swirling jet is a three-dimensional flow different from the straight one. The axial velocity u of any particle of the swirling jet is perpendicular to v and w; thus, v and w do not produce an axial recoil force. According to the law of mass conservation, the total flow rate q_x is the sum of the axial flow rate q_u, radial flow rate q_v, and tangential flow rate q_w. The recoil force of the swirling jet acting on the jet bit is only related to q_u and can be expressed as

$$F_x = 0.745 q_u \sqrt{p_i} \quad (4)$$

The axial velocity distribution along the radial of the swirling jet is approximately shaped as "M"; therefore, for ease of calculation, we can assume that all fluid particles of the swirling jet are distributed on the cone with a diffusion angle of θ_x. Moreover, the approximate relationship between the axial velocity flow rate (q_u) and total flow rate (q_x) can be obtained:

$$q_u = q_x \cos\frac{\theta_x}{2}. \quad (5)$$

Additionally, q_x is

$$q_x = 2.1\mu_f d_x^2 \sqrt{p_i}. \quad (6)$$

Combining Equations (4), (5), and (6), we obtain

$$F_x = 1.56\mu_f \left(d_f^2 - d_m^2\right) p_i \cos\frac{\theta_x}{2}. \quad (7)$$

Finally, the forward nozzle recoil force is

$$F_f = F_m + F_x = 1.56\mu_f p_i \left[d_m^2 + \left(d_f^2 - d_m^2\right)\cos\frac{\theta_x}{2}\right]. \quad (8)$$

2.1.2. Recoil Force of Backward Nozzles. Referring to the analysis method in the previous section, the equation for the backward nozzle recoil force can be written as

$$F_b = \sum_{b=1}^{n_b} 1.56\mu_b d_b^2 p_i \cos\theta_b, \quad (9)$$

where n_b is the number of backward nozzles and d_b, θ_b, and μ_b are the diameter, inclination angle, and flow coefficient of a backward nozzle, separately.

Combining Equations (8) and (9), the self-propelled force of the SSMJ bit can be obtained:

$$F_p = 1.56 p_i \left[\sum_{b=1}^{n_b} \mu_b d_b^2 \cos\theta_b - \mu_f d_m^2 - \mu_f\left(d_f^2 - d_m^2\right)\cos\frac{\theta_x}{2}\right]. \quad (10)$$

2.2. Pressure of the External Fluid on the Bit. In the axial direction, the drill bit is subjected to the pressure of the fluid in the hole on the front end face. The following equation of this pressure F_o is obtained:

$$F_o = \frac{\pi}{4} p_o \left(d_o^2 - d_f^2\right), \quad (11)$$

where d_o is the outer diameter of the bit (mm) and p_o is the pressure of the external fluid on the front end face of the bit (MPa). To be specific, p_o is the sum of the annulus pressure loss and ground pressure, and the ground pressure is 0; thus, the value of p_o is the annulus pressure loss, which can be calculated according to the relevant research [14].

2.3. Friction Resistance of the System. The friction resistance (F') of the RJD system primarily includes the friction between the diverter and hose (F_{rz}), the friction between the borehole and the hose (F_{rk}), and the friction between the borehole and the bit (F_{xk}). Of these, F_{rz} can be obtained through a laboratory test, while

$$F_{rk} = \mu_{rk} G_r l_{rk},\ F_{xk} = \mu_{xk} G_x, \quad (12)$$

where μ_{rk} is the friction coefficient between the hose and borehole, G_r is the submerged weight of a unit length of the hose (N/m), l_{rk} is the friction section length of the hose (m), μ_{xk} is the friction coefficient between the bit and borehole, and G_x is the submerged weight of the jet bit (N).

Substituting Equations (10), (11), and (12) into (1), the force model of the RJD system can be obtained:

$$F = 1.56 p_i \left[\sum_{b=1}^{n_b} \mu_b d_b^2 \cos\theta_b - \mu_f d_m^2 - \mu_f\left(d_f^2 - d_m^2\right)\cos\frac{\theta_x}{2}\right] - \frac{\pi}{4} p_o \left(d_o^2 - d_f^2\right) - F_{rz} - \mu_{rk} G_r l_{rk} - \mu_{xk} G_x. \quad (13)$$

2.4. Pressure Loss of the System. We need to calculate the pressure loss of the RJD system to obtain the inlet pressure of the bit (p_i). Ignoring the leakage at the joint and the local pressure loss such as hose diameter variation and bending, the system pressure loss is primarily generated by the coiled tubing (Δp_{cti}) and the high-pressure hose (Δp_r):

$$p_i = p_b - \Delta p_{cti} - \Delta p_r, \quad (14)$$

where p_b is the pump pressure (MPa).

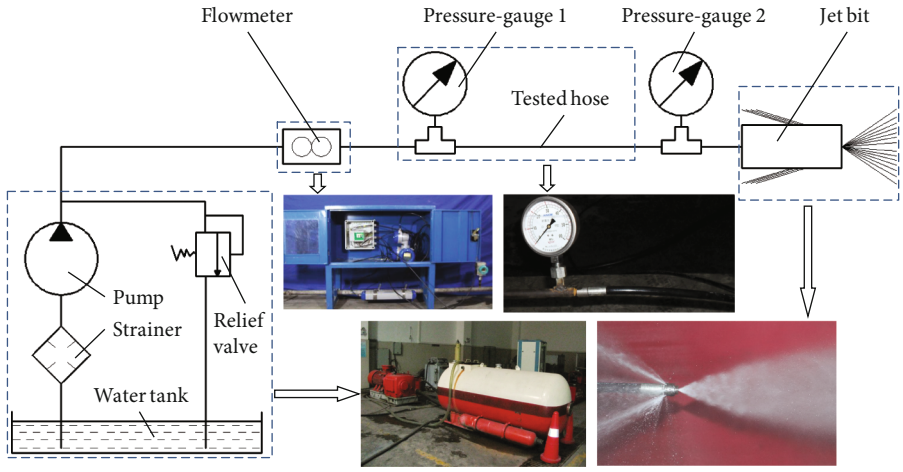

Figure 2: Schematic of the test system.

2.4.1. Theoretical Pressure Loss. The pressure loss along the coiled tubing Δp_{cti} includes the spiral section loss Δp_{cti1} and straight section loss Δp_{cti2}, i.e., $\Delta p_{cti} = \Delta p_{cti1} + \Delta p_{cti2}$, which can be obtained from the previous studies [14].

The theoretical pressure loss of the hose can be obtained using the following equation [28]:

$$\Delta p_r = K_r \times \frac{59.7 q^2 l_r}{d_{ri}^5 \, \mathrm{Re}^{0.25}}, \tag{15}$$

where $K_r = 1$, d_{ri} is the hose inner diameter (mm), q is the volume flow rate (L/min), l_r is the total length of the hose (m), and Re is the Reynolds number, which should be written as $\lambda q / d_{ri}$, and the coefficient λ is 1.12×10^4 under turbulent condition. According to the previous studies [14], the theoretical value of hose pressure loss is quite deviation from the actual, and then, it will greatly affect the judgment of the inlet pressure value of the bit. The correction of Equation (15) is necessary to be performed through an experimental test.

2.4.2. Experimental Test. In this study, several groups of tests were executed under different factors of the flow rate, hose inner diameter, and length; then, the measured pressure loss values under different factors were obtained; moreover, the parameters under each factor were substituted into Equation (15) to obtain the calculated value. By comparing the measured and calculated values, the correction factor K_r is introduced to Equation (15), and the deviation of K_r is analyzed to evaluate the effectiveness of the test. Eventually, K_r is taken as an average value.

The following apparatuses were used (Figure 2): a high-pressure pump, an SSMJ bit, high-pressure hoses of 1/4" (inner diameter of 6.35 mm) and 3/8" (inner diameter of 8 mm), a flowmeter, and two pressure gauges. The two gauges were, respectively, allocated at the inlet and outlet of the tested hose; therefore, the difference reading between pressure gauges No.1 and No.2 was the pressure loss value of the hose when the system operated steadily. The test results are listed in Table 1. K_r is introduced to correct Equation (15). The values of K_r under different conditions range from 0.23 to 0.27, with the relative standard deviation of 1.3%. A small deviation rate proves the effectiveness of the test; then, the final correction factor is taken as an average value, i.e., $K_r = 0.25$.

2.5. Mathematical Model of the Extension Limit. When the resultant force $F > 0$, the RJD system can continuously drill forward. As the drilled radial borehole length increases, the friction increases and F decreases gradually until $F = 0$. Herein, the system is in an equilibrium condition of forces and the bit will not continue to drill forward with the hose; eventually, the value l_{rk} under this condition is exactly the extension limit of the RJD system. Substituting $F = 0$ into Equation (13), we can obtain the prediction model of the extension limit L_{EL}:

$$L_{EL} = \frac{1.56 p_i \left[\sum_{b=1}^{n_b} \mu_b d_b^2 \cos\theta_b - \mu_f \left(d_m^2 + \left(d_f^2 - d_m^2\right) \cos\left(\theta_x/2\right)\right)\right] - (\pi/4) p_o \left(d_o^2 - d_f^2\right) - F_{rz} - \mu_{xk} G_x}{\mu_{rk} G_r}. \tag{16}$$

3. Results and Discussion

3.1. Project Setting. A field construction condition of an oil well in Eastern Sichuan, China, with a radial well depth of 1500 m and casing model of 7" (inner diameter of 168.6 mm) was selected as the analyzed case of this study, and the working pressure of the field pump is 60 MPa. A pure water jet, with a temperature of approximately 90°C

Table 1: Test data of the high-pressure hoses.

Hose length (m)	Hose inner diameter (mm)	Flow rate (L/min)	Tested Δp_r (MPa)	Calculated Δp_r (MPa)	Correction factor Kr
10	6.35	117	10.8	41.68	0.26
10	6.35	55	2.8	11.18	0.25
20	6.35	117	20.0	83.35	0.24
20	6.35	55	5.6	22.35	0.25
10	8	117	3.4	13.13	0.26
10	8	55	0.8	3.52	0.24
20	8	117	7.1	26.26	0.27
20	8	55	1.6	7.04	0.23

Table 2: Main parameters of the project.

l_{ct} (m)	d_{cto} (mm)	d_{cti} (mm)	l_r (m)	d_{ro} (mm)	d_{ri} (mm)	G_r (N/m)	ρ_z (g/cm^3)	l_z (mm)	d_o (mm)	d_i (mm)	d_f (mm)	d_m (mm)	θ_x (°)	n_b	d_b (mm)	θ_b (°)
2000	38.1	31.75	120	14.3	8	2.3	15	30	18	8	1.8	1	60	3	1.3	30

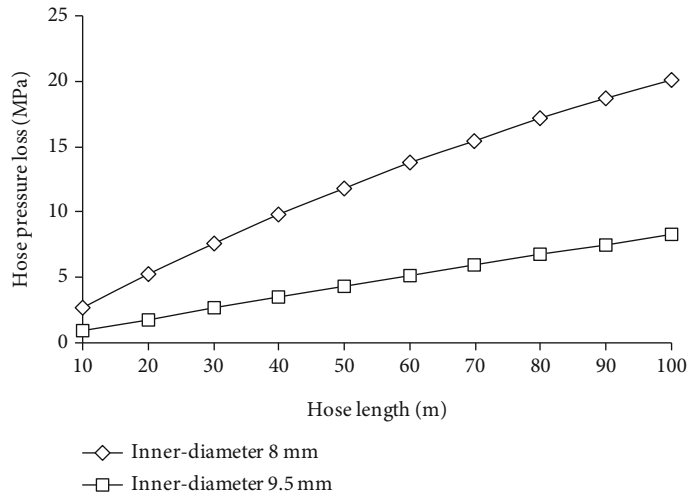

Figure 3: Hose pressure loss influenced by the hose length.

under this operating condition, a density of 965.4 kg/m^3, and a viscosity of 0.315×10^{-3} Pa·s, was used. A drilling experiment using an SSMJ bit has been executed previously; then, a borehole with a diameter of 25 mm was obtained, and μ_{rk} and μ_{zk} are both 0.3. According to experience and the previous laboratory tests, the flow coefficients of the forward and backward nozzles μ_f and μ_b are both set as 0.83; furthermore, the friction between the hose and diverter F_{rz} was obtained as 20 N through a ground test.

A coiled tubing with a model of 1.5" was used, and its main parameters of length l_{ct} and outer and inner diameter d_{cto} and d_{cti} are shown in Table 2; additionally, Table 2 shows the length l_r and outer and inner diameter d_{ro} and d_{ri} and submerged weight G_r of high-pressure hose with a model of 5/16"; the self-propelled bit was made by cemented carbide, and its specific dimensions are also shown in Table 2, such as density ρ_z, length l_z, outer diameter d_o, inner diameter d_i, forward nozzle diameter d_f, impeller central hole diameter d_m, jet diffusion angle θ_x, number of backward nozzles n_b, diameter of backward nozzle d_b, and inclination angle of backward nozzle θ_b.

3.2. Pressure Loss Analysis. The construction parameters were substituted into Ma et al.'s study [14] and Equation (15) to obtain the pressure loss distribution along the coiled tubing and high-pressure hose, separately. The main pressure loss of the system was observed to emanate from the high-pressure hose, which was 20.1 MPa, accounting for 92.6% of the total.

The hose parameters (inner diameter d_{ri} and length l_r) have a significant impact on the pressure loss (Figure 3). The pressure loss increases as a quadratic function with the increase in l_r, which will reduce the extension limit. Therefore, the length of the hose should be as short as possible. During engineering construction, l_r must be chosen according to the designed radial borehole length, and a little longer than the designed borehole length should be most suitable. The pressure loss is highly sensitive to the variation in d_{ri}; therefore,

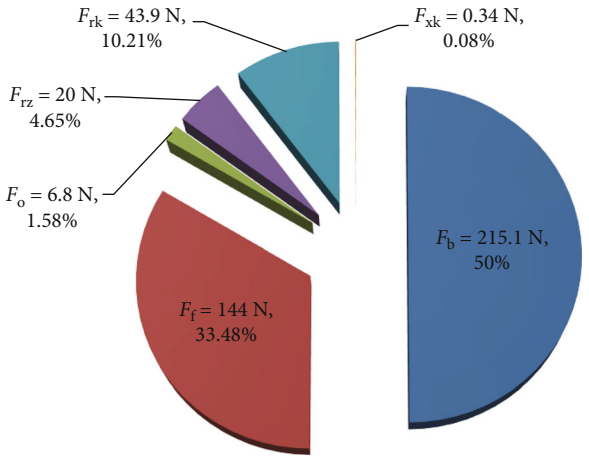

Figure 4: Force distribution of the RJD system.

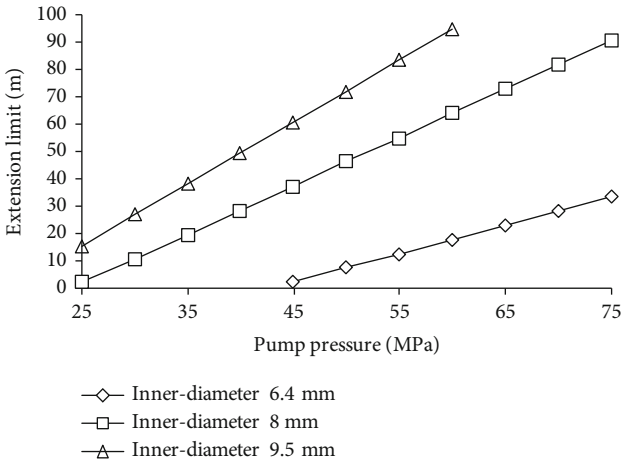

Figure 5: Extension limit influenced by the pump pressure.

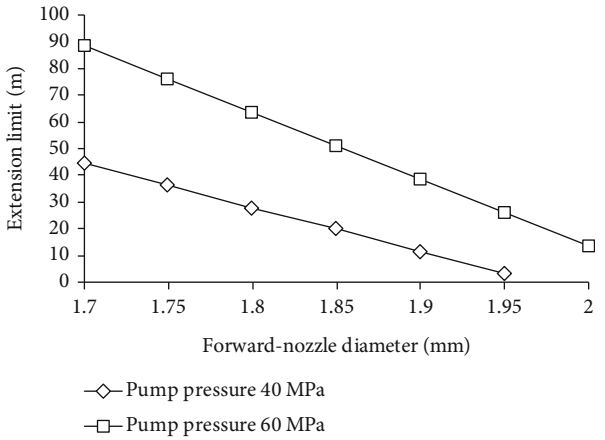

Figure 6: Extension limit influenced by the forward nozzle diameter.

d_{ri} should be as large as possible, provided that the high-pressure hose can smoothly pass through the diverter.

3.3. Extension Limit Results and Analysis. The construction parameters of an oil well in Eastern Sichuan were placed into Equation (16), and the extension limit of the RJD system L_{EL} was calculated as 63.7 m. The force distribution in the horizontal section of RJD is shown in Figure 4. We observe that the recoil force (F_b) of the backward nozzle is the sole driving force for the system to drill forward; thus, increasing the equivalent diameter of the backward nozzles (any nozzle diameter or number) is the most effective method of increasing the drilling depth. The recoil force (F_f) of the forward nozzle is the main resistance of the system, accounting for 66.96% of the total resistance. Therefore, the diameter of the forward nozzle should be appropriately reduced, provided that its rock-breaking performance satisfies the design requirements. The friction between the hose and borehole (F_{rk}) increases with the increase in drilling depth. When the axial force of the system is balanced, F_{rk} also reaches the maximum. Herein, F_{rk} accounts for 20.42% of the total resistance. A hose with a light weight and smooth outer surface should be selected to reduce F_{rk}. In the bit structure design, the roundness of the drilled hole is used as an evaluation index. The friction between the hose and diverter (F_{rz}) accounts for 9.3% of the total resistance. A hose with a small turning radius should be selected in a RJD system to reduce F_{rz}. In the design of diverter, the hose and bit should be investigated on whether they can pass through the diverter smoothly.

3.4. Influential Factor Analysis for Extension Limit

3.4.1. Pump Pressure. We changed the pump pressure p_b and maintained other parameters in the engineering example to obtain the variation law of extension limit L_{EL} with p_b under different inner diameters of the hose (Figure 5). We observed that the extension limit increases approximately linearly with the increase in p_b. Besides, the inner diameter of the high-pressure hose has a significant influence on L_{EL}. When the inner diameter is 6.4 mm, the drill bit can drag the high-pressure hose forward after p_b reaches 45 MPa, whereas when the diameter is 8 mm, the drill bit can drag the high-pressure hose forward when p_b reaches 25 MPa. The larger the inner diameter, the greater the slope, additionally the higher the rise rate of L_{EL}, which indicates that the increase in the inner diameter of the hose can effectively reduce the pressure loss and improve the inlet pressure of the bit.

3.4.2. Forward Nozzle Diameter. We changed the forward nozzle diameter (d_f) and maintained other parameters in the engineering example to obtain the variation law of L_{EL} (Figure 6). We observed that when the pump pressure is 60 MPa, the decline rate of L_{EL} is greater than that when 40 MPa. This is because when the pump pressure is relatively high, the flow rate of the system is relatively large. As d_f increases, the increase rate of the system pressure loss is also faster, which increases the decline rate of the nozzle inlet pressure compared with when the pump pressure is relatively low, and finally increases the decline rate of the drilling extension limit. Under the same pump pressure, L_{EL} decreases approximately linearly with the increase in d_f;

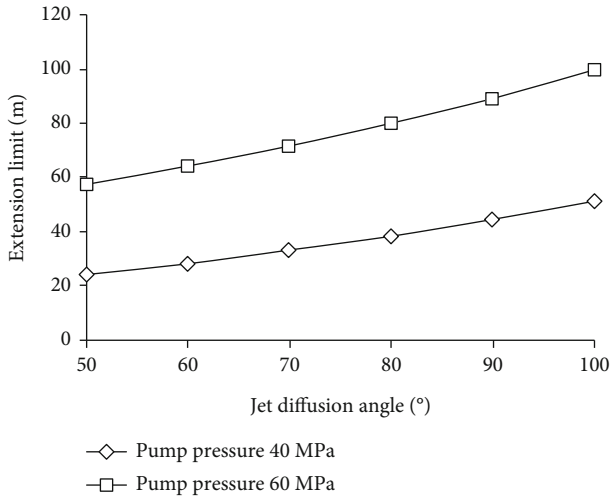

Figure 7: Extension limit influenced by the diffusion angle.

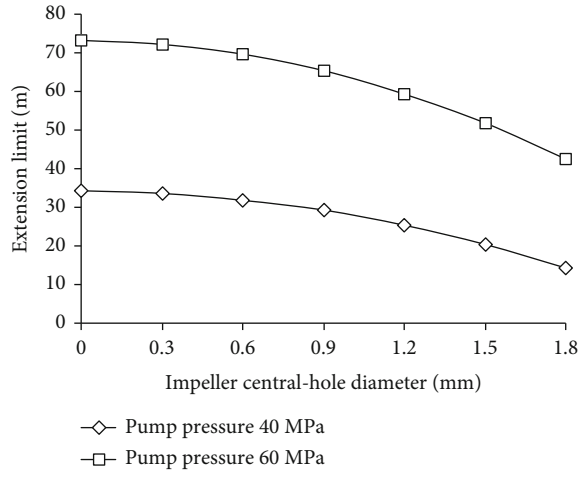

Figure 8: Extension limit influenced by the impeller central hole.

therefore, reducing the diameter of the forward nozzle is conducive to increasing L_{EL}. However, the main function of the forward nozzle is to generate an SSMJ for rock-breaking to enable the system to continuously drill forward. The smaller diameter of the forward nozzle weakens the energy of the jet and the rock-breaking performance of the bit becomes worse. Therefore, when selecting d_f, we should also combine with rock-breaking research and appropriately reduce d_f under the premise that the rock-breaking efficiency satisfies the operating requirements.

3.4.3. Jet Diffusion Angle. We changed the jet diffusion angle (θ_x) by adjusting the slot dip angle of the impeller and maintained other parameters in the engineering example to obtain the variation law of L_{EL} (Figure 7). We observed that under the same pump pressure, L_{EL} increases as a cosine curve with the increase in θ_x. By increasing θ_x, the axial velocity of the swirling jet decreases, and then, the recoil force of the forward nozzle decreases. The decrease in the system resistance can improve L_{EL} of the system, but an excessively large diffusion angle will also weaken the rock-breaking efficiency of the SSMJ. Therefore, the flow field and erosion performance analysis must be combined to obtain the optimal θ_x.

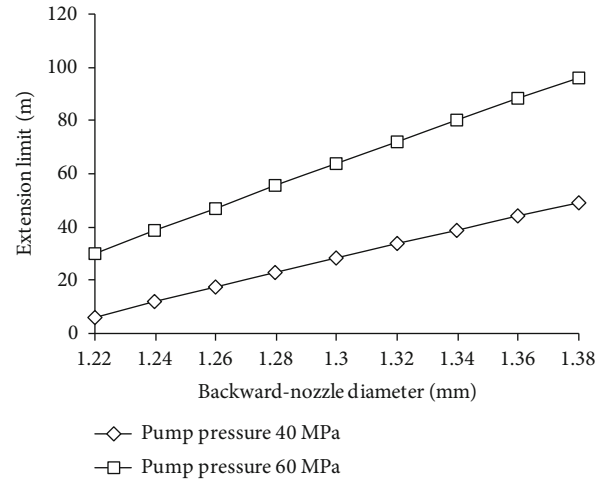

Figure 9: Extension limit influenced by the backward nozzle diameter.

3.4.4. Impeller Central Hole Diameter. The variation law of L_{EL} was obtained by changing the diameter of the impeller central hole d_m (Figure 8). Under the same pump pressure, L_{EL} decreases in a quadratic function with the increase in d_m. Therefore, the diameter can be appropriately reduced to increase L_{EL}. However, according to the previous research, when d_m is small, the central boss easily appears in the borehole bottom, which hinders the advancement of the bit and reduces the drilling speed. Therefore, the size of the central hole should satisfy the larger L_{EL} and drilling speed. When d_m is greater than 1.5 mm, L_{EL} decreases to a lower value, and the decline rate reaches 40% under the pump pressure of 60 MPa. Thus, d_m less than 1.5 mm is more appropriate; additionally, the specific results can be further investigated combining the drilling efficiency test.

3.4.5. Backward Nozzle Diameter. We changed the backward nozzle diameter (d_b) and maintained other parameters in the engineering example to obtain the variation law of L_{EL} (Figure 9). Under the same pump pressure, L_{EL} increases approximately linearly with the increase in d_b. According to the data, the increase rate of L_{EL} decreases with the increase in d_b. For example, under the condition of a pump pressure of 60 MPa, when d_b changes from 1.22 to 1.24 mm, L_{EL} increases by 8.55 m, whereas for a d_b changes from 1.36 to 1.38 mm, L_{EL} increases by 7.85 m. Increasing d_b is the most effective method of increasing the drilling depth. However, at the same pump pressure, the increase in d_b increases the flow rate, additionally increases the water consumption and pressure loss of the system, and reduces the increase rate of L_{EL}. Therefore, considering the system loss and economy, d_b cannot increase indefinitely and should be determined according to the drilling extension limit required by the construction design.

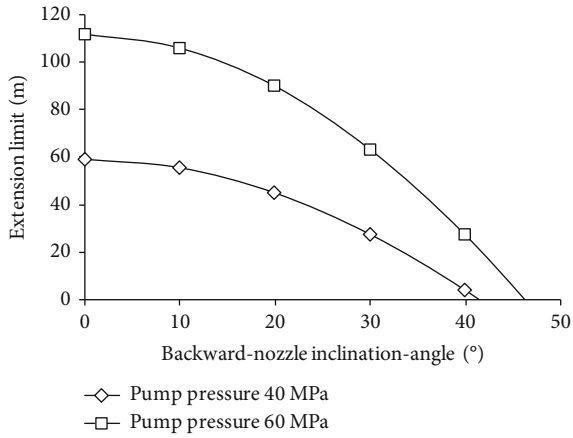

Figure 10: Extension limit influenced by the backward nozzle inclination angle.

3.4.6. Backward Nozzle Inclination Angle. We changed the inclination angle of the backward nozzle (θ_b) to obtain the variation law of L_{EL} (Figure 10). Under the same pump pressure, L_{EL} decreases as a cosine function with an increase in θ_b. Except for providing the SSMJ a driving force, the backward nozzle also has the function of reaming. Reducing θ_b is conducive to increasing L_{EL}, but its reaming capacity decreases, and too small θ_b will cause the fluid to erode the high-pressure hose. According to the prediction model of L_{EL}, when the pump pressure is 60 MPa and θ_b is 0, L_{EL} is 111.91 m. When θ_b increases to 20°, 30°, and 40°, L_{EL} decreases to 90.20, 63.68, and 27.69 m, respectively. When θ_b reaches 48.4°, L_{EL} is 0. Overall, L_{EL} decreases relatively rapidly when θ_b exceeds 30°. Therefore, it is reasonable to select θ_b of 30° to ensure both a large L_{EL} and borehole diameter.

3.5. Parameter Sensitivity Analysis. In this study, the method of grey relational analysis (GRA) was used to investigate the influence degree of six factors above on the extension limit, such as pump pressure p_b, forward nozzle diameter d_f, jet diffusion angle θ_x, impeller central hole diameter d_m, backward nozzle diameter d_b, and backward nozzle inclination angle θ_b. GRA refers to the uncertain correlation between objects or between subsystems and between factors and main behavior. Its basic assignment is to analyze and determine the influence degree between factors or the contribution degree of factors to main behavior, based on the micro or macro geometric proximity of behavior factor sequences. The detailed calculation process is as follows:

(1) Determine the reference and comparison sequences: taking the reference sequence reflecting the characteristics of system behavior as y, and the comparison sequence affecting system behavior as x_i, the corresponding equation is as follows:

$$\begin{cases} y = \{y(k) | k = 1, 2, \cdots, n\}, \\ x_i = \{x_i(k) | k = 1, 2, \cdots, n\}, \end{cases} \tag{17}$$

where k and i are the group k and column i of a specific quantity value in the matrix composed of sequences, $y(k)$ is the reference sequence value of the data group k and its unit is related to the chosen physical quantity, and $x_i(k)$ is the value of the i'th influential factor of data group k and its unit is also related to the selected physical quantity

(2) Dimensional normalization processing of the data: it is necessary to unify the unit for different parameters, usually the dimensional normalization methods including mean value, initial value, maximization, and minimization. The initial value method was adopted, since it is suitable for the data with a tendency and regularity and is often used in comprehensive evaluation, such as GRA

(3) Calculation of relation coefficient: the equation is as follows:

$$\xi_i(k) = \frac{\min\limits_i \min\limits_k |x_0(k) - x_i(k)| + \rho \bullet \max\limits_i \max\limits_k |x_0(k) - x_i(k)|}{|x_0(k) - x_i(k)| + \rho \bullet \max\limits_i \max\limits_k |x_0(k) - x_i(k)|}, \tag{18}$$

where ρ is the resolution coefficient and has a value range between 0 and 1, usually as 0.5. The smaller ρ, the greater the difference between relation coefficients, and the stronger the discrimination ability. After calculating the relation coefficient, take the average value of each coefficient as the grey relation coefficient of the factor, and the calculation equation is

$$r_i = \frac{1}{n} \sum_{k=1}^{n} \xi_i(k), \tag{19}$$

where r_i is the relation degree of the i'th influential factor

Take the extension limit L_{EL} of the jet bit under different parameters as the reference sequence, which is y_o, and take p_b, d_f, θ_x, d_m, d_b, and θ_b as the comparison sequence, which are x_1 to x_6, respectively. It is found that taking L_{EL} as the

Table 3: Calculation results.

Comparison sequence	Relation coefficient	Sensitivity order
p_b	0.52963	1
θ_x	0.51874	2
d_f	0.51867	3
d_b	0.51856	4
θ_b	0.51852	5
d_m	0.51842	6

evaluation index, the order of parameter sensitivity from large to small is p_b, θ_x, d_f, d_b, θ_b, and d_m (Table 3).

4. Conclusions

Through analysing the force and pressure loss of the RJD system, a model to predict the drilling extension limit L_{EL} was established. The L_{EL} value of a specific project was calculated and the pressure loss and forces were obtained. The influence laws of the main parameters on L_{EL} were studied using the established prediction model. The conclusions are summarized as follows:

(1) The sensitivity of pressure loss to the variation in the inner diameter is higher, because the diameter of high-pressure hose is significantly lower than that of the coiled tubing, and the main pressure loss of the system results from the high-pressure hose. The backward nozzle recoil force is the only driving force of the system, and the forward nozzle recoil force and friction between the hose and borehole contain the main resistance of the system. The drilling extension limit prediction value of the project in this article can reach up to 63.7 m

(2) Under the same pump pressure, L_{EL} of the system increases approximately linearly with the increase in backward nozzle diameter, yet this will significantly increase hydraulic consumption and pressure loss; it decreases linearly with the increase in the forward nozzle diameter. Therefore, the design of the rear nozzle should not blindly pursue the large L_{EL} but also consider that the hydraulic consumption and pressure loss are within a reasonable range; the forward nozzle diameter can be as small as possible on the premise of ensuring rock-breaking efficiency. L_{EL} increases with the increase in the swirling jet diffusion angle; the diffusion angle can also be reduced to ensure the capability of rock-breaking rock. L_{EL} decreases as a quadratic function with the increase in the backward nozzle installation angle; when the angle is larger than 30°, the decrease in L_{EL} rate is high. From parameter sensitivity analysis, the factors that have the greatest and least influence on L_{EL} are p_b and d_m, respectively. Hence, increasing p_b is the most direct and effective way to raise L_{EL}, while the design of d_m does not depend on the requirements of L_{EL}, but on its rock-breaking capacity

(3) This research provides a theoretical guideline for predicting the extension limit of RJD under a specific working condition, optimizing the bit structure, and choosing high-pressure hose and hydraulic parameters. The specific bit structure parameters should be further obtained through rock-breaking performance tests combined with this study. In addition, laboratory simulation of RJD experiment and field test will be performed in the future

Data Availability

All data generated or used during the study appearing in the submitted article are available from the corresponding author upon request.

Conflicts of Interest

The authors declared no potential conflicts of interest with respect to the research, authorship, and/or publication of this article.

Acknowledgments

This study was financially supported by the National Natural Science Foundation of China (NSFC) under Grant No. 51804007.

References

[1] Y. Li, Z. S. Wang, S. H. Tang, and D. Elsworth, "Re-evaluating adsorbed and free methane content in coal and its ad- and desorption processes analysis," *Chemical Engineering Journal*, vol. 428, article 131946, 2022.

[2] Y. Qin, T. A. Moore, J. Shen, Z. Yang, Y. Shen, and G. Wang, "Resources and geology of coalbed methane in China: a review," *International Geology Review*, vol. 60, no. 5-6, pp. 777–812, 2018.

[3] R. M. Flores, *Coal and Coalbed Gas: Fueling the Future*, Elsevier Science Publishing Co Inc, United States, 2014.

[4] Y. Li, J. Yang, Z. Pan, S. Meng, K. Wang, and X. Niu, "Unconventional natural gas accumulations in stacked deposits: a discussion of Upper Paleozoic coal-bearing strata in the east margin of the Ordos Basin, China," *Acta Geologica Sinica-English Edition*, vol. 93, no. 1, pp. 111–129, 2019.

[5] Y. Li, Z. Wang, Z. Pan, X. Niu, Y. Yu, and S. Meng, "Pore structure and its fractal dimensions of transitional shale: a cross-section from east margin of the Ordos Basin, China," *Fuel*, vol. 241, pp. 417–431, 2019.

[6] W. Dickinson and R. W. Dickinson, "Horizontal radial drilling system," in *Presented at the SPE California Regional Meeting*, pp. 27–29, Bakersfifield, California, 1985.

[7] Y. Li and T. Zhang, "Investigation of the factors affecting the self-propelled force in a multi-orifice nozzle using a novel simulation method," *Energy Science and Engineering*, vol. 8, no. 9, pp. 3136–3147, 2020.

[8] Y. Y. Lu, Z. Zhou, Z. L. Ge, X. W. Zhang, and Q. Li, "Research on and design of a self-propelled nozzle for the tree-type drilling technique in underground coal mines," *Energies*, vol. 8, no. 12, pp. 14260–14271, 2015.

[9] X. L. Li, S. J. Chen, S. Wang, M. Zhao, and H. Liu, "Study on in situ stress distribution law of the deep mine: taking Linyi mining area as an example," *Advances in Materials Science and Engineering*, vol. 2021, Article ID 5594181, 11 pages, 2021.

[10] D. Z. Dong, C. N. Zhou, J. Z. Li, S. J. Wang, X. Li, and J. L. Huang, "Resource potential, exploration and development prospect of shale gas in the whole world," *Geological Bulletin of China*, vol. 30, no. 2, pp. 324–336, 2011.

[11] A. Kochnev, S. Galkin, S. Krivoshchekov, N. Kozyrev, and P. Chalova, "Application of machine learning algorithms to

predict the effectiveness of radial jet drilling technology in various geological conditions," *Applied Sciences*, vol. 11, no. 10, p. 4487, 2021.

[12] A. M. Ragab and A. M. Kamel, "Radial drilling technique for improving well productivity in petrobel-Egypt," in *Proceedings of the North Africa Technical Conference and Exhibition*, Held in Cairo, Egypt, 2013.

[13] P. Buset, M. Riiber, and A. Eek, "Jet drilling tool: cost-effffective lateral drilling technology for enhanced oil recovery," in *Paper SPE 68504 Presented at the SPE/ICoTA Coiled Tubing Round table*, Houston, Texas, USA, 2001.

[14] D. J. Ma, G. S. Li, and Z. W. Huang, "A model of calculating the circulating pressure loss in coiled tubing ultra-short radius radial drilling," *Petroleum Exploration and Development*, vol. 39, no. 4, pp. 528–533, 2012.

[15] T. Zhang, Y. Li, H. Lu, and J. Jiang, "Simulation and experimental study on characteristics of multiorifice nozzle in radial jet drilling," *Geofluids*, vol. 2022, Article ID 2531181, 8 pages, 2022.

[16] Y. Y. Lu, Y. Liu, X. H. Li, and Y. Kang, "A new method of drilling long boreholes in low permeability coal by improving its permeability," *International Journal of Coal Geology*, vol. 84, no. 2, pp. 94–102, 2010.

[17] D. J. Ma, G. S. Li, J. L. Niu, H. L. Liao, and Z. W. Huang, "Experimental study on rock breaking and drilling laws by multi-hole jet bit," *Fluid Mach*, vol. 43, no. 3, pp. 1–5, 2015.

[18] Y. Tang, P. Sun, G. R. Wang, B. W. Fu, and J. X. Yao, "Rock-breaking mechanism and efficiency of straight-swirling mixed nozzle for the nondiagenetic natural gas hydrate in deep-sea shallow," *Energy Science & Engineering*, vol. 8, no. 10, pp. 3740–3752, 2020.

[19] J. B. Li, G. S. Li, Z. W. Huang, X. Z. Song, R. R. Yang, and K. W. Peng, "The self-propelled force model of a multi-orifice nozzle for radial jet drilling," *Journal of Natural Gas Science and Engineering*, vol. 24, pp. 441–448, 2015.

[20] J. B. Li, J. C. Dai, Z. W. Huang, G. Zhang, X. Liu, and H. Li, "Rock breaking characteristics of the self-rotating multi-orifice nozzle for sandstone radial jet drilling," *Rock Mechanics and Rock Engineering*, vol. 54, no. 11, pp. 5603–5615, 2021.

[21] Y. B. Liu, Q. B. Ba, L. P. He, K. Shen, and W. Xiong, "Study on the rock-breaking effect of water jets generated by self-rotatory multinozzle drilling bit," *Energy Science & Engineering*, vol. 8, no. 7, pp. 2457–2470, 2020.

[22] P. Du, Y. Y. Lu, J. R. Tang, H. Zhou, and W. F. Zhang, "Characteristics and mechanism of rock breaking for new type straight-swirling integrated jet," *Journal of Xi'an Jiaotong University*, vol. 50, no. 3, pp. 81–89, 2016.

[23] W. G. Buckman, *Method and Apparatus for Jet Drilling Drainholes from Wells*, U.S. Patent 6, 263, 984 B1, 2001.

[24] D. J. Ma, G. S. Li, X. N. Zhang, and Z. W. Huang, "Experimental study on rock breaking by a combined round straight jet with a swirling jet nozzle," *Atomization and Sprays*, vol. 21, no. 8, pp. 645–653, 2011.

[25] H. L. Liao, G. S. Li, J. L. Niu, and Z. W. Huang, "Integrating straight & swirling jets bit design and its rock breaking characteristics for radial horizontal hole drilling," *Journal of China Coal Society*, vol. 38, no. 3, pp. 424–429, 2013.

[26] I. Toh, D. Honnery, and J. Soria, "Velocity and scalar measurements of a low swirl jet," in *Fourth Australian Conference on Laser Diagnostics in Fluid Mechanics and Combustion, The University of Adelaide*, pp. 129–132, South Australia, Australia, 2005.

[27] Z. H. Shen, *Water Jet Theory and Technology*, Petroleum University Publishing House, Dongying, Shandong, China, 1998.

[28] T. J. Labus, *Fluid Jet Technology: Fundamentals and Application*, Water Jet Technology Association, St. Louis, MO, USA, 1995.